Abridged version

KAWASAKI STEEL TECHNICAL REPORT
No.16 ( June 1987 )

# Development of Automatic Process Control System for a 7" Seamless Tube Mill

Yutaka Funyu, Tadashi Okumura, Norio Konya, Yasuyuki Hayashi, Hiromu Oka, Toshio Imae

Synopsis :
New process computer system has been developed at the 7" seamless tube mill of Chita Works following the 16" seamless tube mill. The former system has realized highly automated control for each mill through the development of on-line gages and rolling control models. Optimal control model for the piercer, cross section profile control model for mandrel mill and adaptive elongation control model for the stretch reducer are mainly described. New bulge gage has been applied to mandrel mill control. The accuracy of the tube dimensions and standardization of rolling operations are markedly improved by applying the high-level software and hardware to rolling process. An outline of the automatic computer control system, its performances and the results of its adoption are discussed in this report.

(c)JFE Steel Corporation, 2003

The body can be viewed from the next page.

# Development of Automatic Process Control System for a 7″ Seamless Tube Mill*


Yutaka Funyu
Staff General Manager, Equipment & Engineering Sec., Chita Works

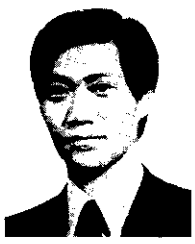

Tadashi Okumura
Staff Manager, Equipment & Engineering Sec., Chita Works

Norio Konya
Equipment & Engineering Sec., Chita Works

Yasuyuki Hayashi
Assistant Manager, Small Seamless Pipe Sec., Pipe Dept., Chita Works

Hiromu Oka
Seamless Pipe Technology Sec., Pipe Dept., Chita Works

Toshio Imae
Senior Researcher, Chita Research Dept., I & S Research Labs.



***Synopsis:***

*New process computer system has been developed at the 7″ seamless tube mill of Chita Works following the 16″ seamless tube mill. The former system has realized highly automated control for each mill through the development of on-line gages and rolling control models. Optimal control model for the piercer, cross section profile control model for mandrel mill and adaptive elongation control model for the stretch reducer are mainly described. New bulge gage has been applied to mandrel mill control. The accuracy of the tube dimensions and standardization of rolling operations are markedly improved by applying the high-level software and hardware to rolling process. An outline of the automatic computer control system, its performances and the results of its adoption are discussed in this report.*


## 1 Introduction

Seamless tube rolling control techniques at Chita Works were first developed around 1978 at the time of constructing the 16″ seamless tube mill, with a numerically-controlled rolling technique firmly established in operation. In 1982, Chita Works introduced a process computer system to its 7″ seamless tube mill, and has since continued the efforts in developing the control technique for rolling.

The introduction of a control system into the existing mills involved many rigorous limiting conditions. In addition, since the 7″ seamless tube mill, contrary to the 16″ one, required fast rolling speed and constituted a complex process consisting of a multistand continuous mill, the development encountered many difficulties. However, through various favorable factors such as technical transfer from the 16″ seamless tube making techniques, active use of ample operation expertise gained in the past, developments of new sensors, and making of accurate control models which reflected model mill experiments, it was possible to construct a highly-developed process-computerized rolling control system in a comparatively short time to establish rolling control techniques at Chita Works. Supported by highly-reliable hardward and software, the control techniques produced noticeable results in the standardization of operation, improvement in quality and productivity, and energy saving. This paper reports an outline of the rolling control system, and the sensors, and control models used in the system.

## 2 Environment of System Development

### 2.1 Layout of Rolling Line

A layout of the rolling line of 7″ seamless tubes is

* Originally published in *Kawasaki Steel Giho*, **18**(1986)2, pp. 160-168

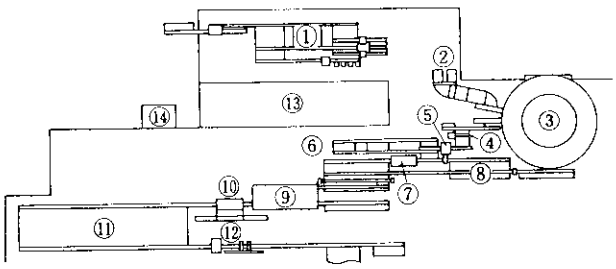

① Billet conditionig line
② Billet charging table
③ Rotary hearth furnace
④ Billet centering machine
⑤ Piercing mill
⑥ Plug circulation system
⑦ Mandrel mill
⑧ Bar circulation system
⑨ Walking beam furnace
⑩ Stretch reducer
⑪ Cooling bed
⑫ Cold saw
⑬ Electric room
⑭ Computer room

Fig. 1 Layout of 7″ seamless tube mill line

shown in **Fig. 1**. Long billets transported from Mizushima Works are cut into smaller billets by the billet cutting line at Chita Works. These cut-out billets are charged into the doughnut-shaped rotary reheating furnace. Each heated billet is pierced by a piercer and becomes a hollow bloom, which in turn is fitted with a mandrel bar and rolled on the 8-stand full-float mandrel mill to become a shell. The mandrel bar, immediately after rolling, is pulled out of the shell and reused in circulation. The shell is reheated and reduced on the 24-stand stretch reducer into a tube of a prescribed outside diameter. The tube is then cooled on the cooling bed and cut into a specified product length by the cold saw. Thus, almost 700 pieces of steel material are staying in the rolling line at all times.

Table 1 Comparison of process features between 7″ and 16″ seamless tube mills

| | Mill type | Elongation ratio | Rolling length (m) | Rolling speed (m/s) | Cycle time (s) | Control loop |
|---|---|---|---|---|---|---|
| 7″ mill | | | | | | |
| Piercing mill | Cross roll | — | 10 | 1.4 | | |
| Mandrel mill | Multi stand | 2.0~4.0 | 26 | 5.5 | 15 | 84 |
| Stretch reducer | Multi stand | 1.0~4.5 | 64 | 7.8 | | |
| 16″ mill | | | | | | |
| Piercing mill | Cross roll | — | 9 | 1.2 | | |
| Elongator | Cross roll | 1.2~2.0 | 13 | 1.2 | | |
| Plug mill | Single stand | 1.1~1.5 | 19 | 3.0 | 25 | 34 |
| Reeler | Cross roll | 1.0 | 19 | 0.9 | | |
| Sizing mill | Multi stand | 1.0 | 19 | 3.0 | | |

### 2.2 Features of Rolling Process

A comparison of rolling processes between 7″ and 16″ seamless tube is shown in **Table 1**. The features of the 7″ seamless tube process are the width of dynamic range of rolling control, a high rolling speed, and a large number of control loops.

The 7″ seamless rolling line was constructed in 1971, and the mechanical and electrical control systems are both two-decade old. It is another feature of the present rolling control system that the system was developed on the basis of such existing facilities.

## 3 Outline of Control System

### 3.1 Functions and Aims

Various functions of the control system which was developed this time are shown in **Fig. 2**. Main functions are

(1) Piece Tracking: Tracking is performed in two ways. One is tracking of materials over the entire processes ranging from billet charging to the rolling line. The other is tracking of tooling such as for the mandrel

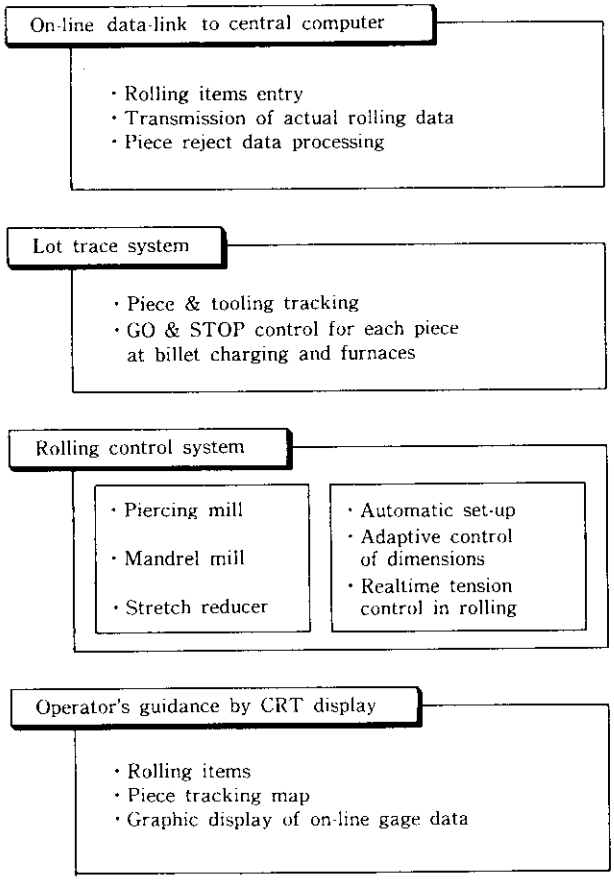


Fig. 2 Functions of computer control system

bars.

(2) Rolling Control of Mill: Adaptive-control and learning models have been developed on the piercer, mandrel mill and stretch reducer using models based on the plasticity theory, thereby achieving full-automatic rolling.

(3) Data Transfer to central computer: The rolling schedule and actual rolling data are mutually handed over between the central computer and the control system.

(4) Operator Guidance: Mill setting values, measured dimensions, and tracking maps are displayed on CRT screens to support operators.

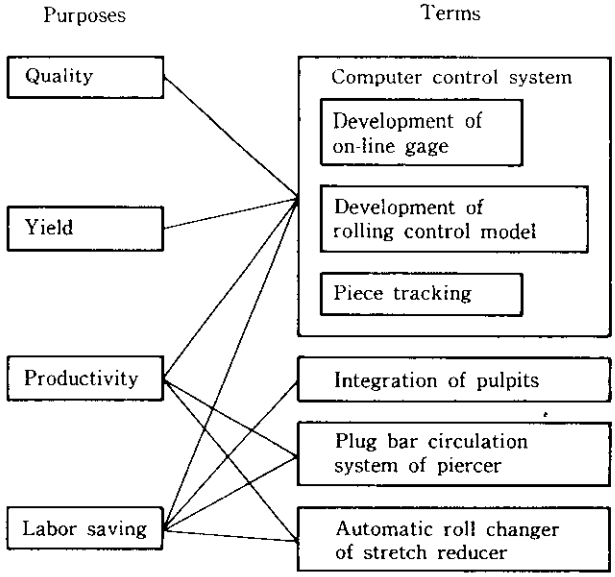


Fig. 3 Purposes of computer control system

Next, tasks which were set up at the time of developing the present control system are shown in **Fig. 3**. Tasks for improving the existing facilities such as unification of the operator rooms and introducing of plug bar circulation of the piercer, which were carried out in parallel to improve the effects of introduction of the control system, are also shown in the figure for reference. The aims of the present system lie in improvement in quality and yield, enhancement of productivity, and labor reduction. In addition, full standardization of operation is important as a basic task.

### 3.2 Hardware Configuration

Taking into consideration the features and functions of the 7″ seamless rolling process, hardware configuration shown in **Fig. 4** was decided. Points taken into con-

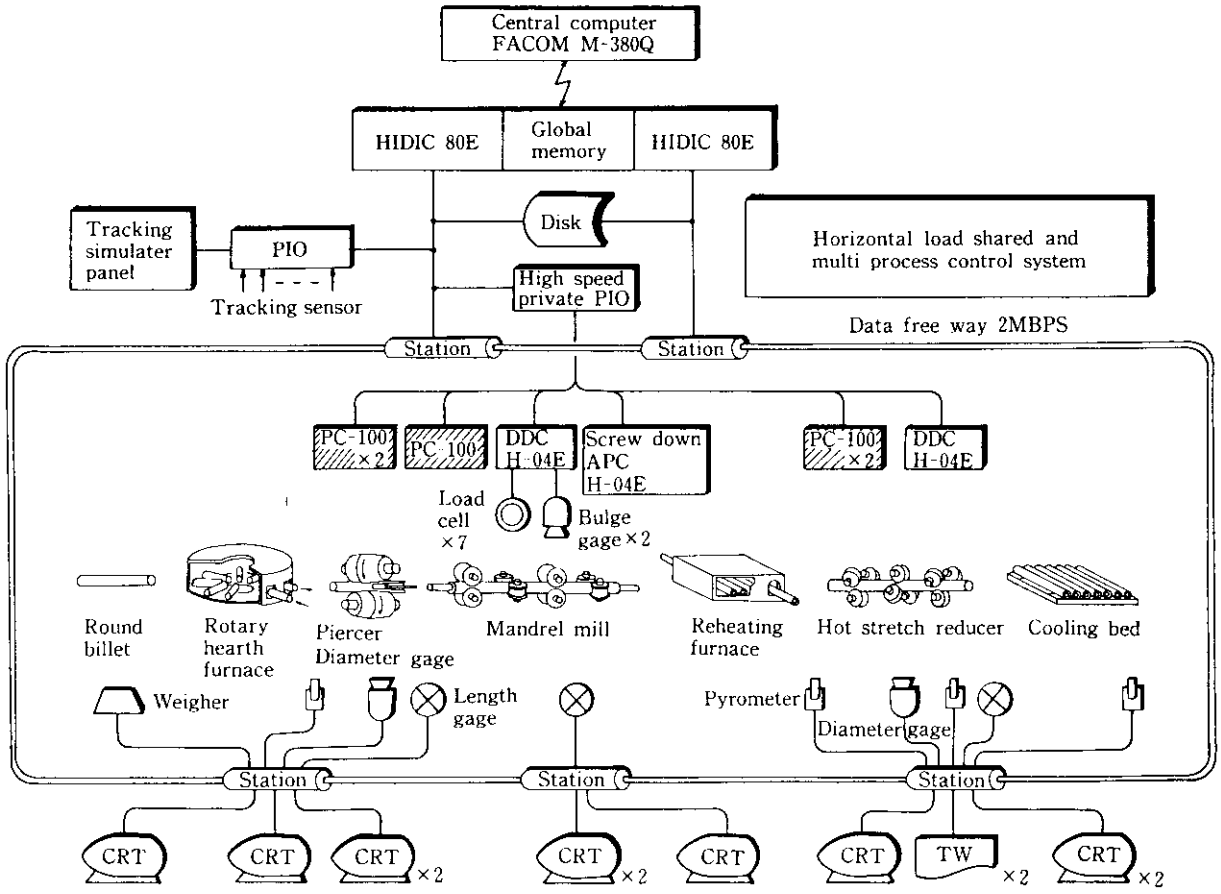


Fig. 4 Basic system configuration of 7″ seamless tube mill

sideration when the hardware configuration was made were as follows:

(1) To reduce process computer load in piece tracking, a horizontal load sharing system, in which the control functions were distributed into the real-time system and off-line system, was adopted.
(2) Sharing of functions between electrical equipment and the process computer was reviewed for achieving simplification.
(3) On-line gages used for inter-piece adaptive control were connected to the data freeway, and on-line gages used for intra-piece optimum control were directly coupled to DDC, thereby permitting optimal sharing of rolling process information within the control system and ensuring real-time control.

Through adoption of the hardware configuration and by paying careful attention to the software configuration, the process computer load factor has never exceeded 60%, even when the rolling line is operated at a cycle time of 15 sec. All control models also respond within 0.3 sec or below.

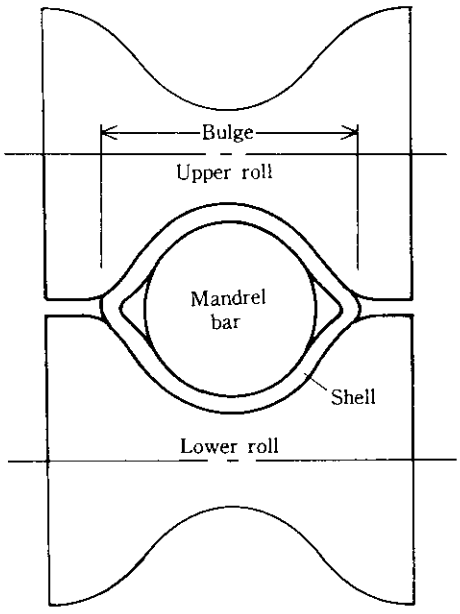


Fig. 5 Cross section profile of shell in rolling at mandrel mill

## 4 Development of On-line Gages

In constructing rolling control system, whether it may be used for seamless steel tubes or other steel products, the use of on-line gages is indispensable. In the present system, on-line gages shown in Fig. 4 were developed and introduced.

To improve the accuracy of the rolling control model, it was considered to correctly measure the bulge width during the mandrel mill rolling as shown in **Fig. 5**, and the development of gages which can satisfy the following conditions was undertaken:

(1) Since the distance between rolling machine housings is 50 mm, the gage must be able to measure within the distance of 50 mm.
(2) When the rolling roll is changed, the entire housing must be changed. Therefore, the gage must not be in the way of the housing changes.
(3) The rolling speed is 5 m/s maximum, and the measured value of the bulge is required at every 200 mm

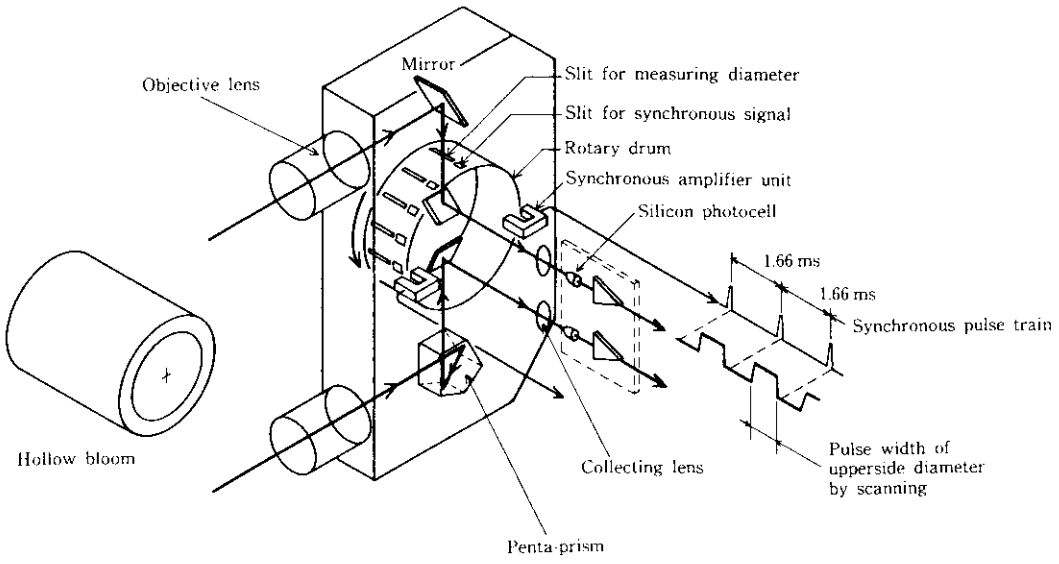


Fig. 6 Schematic structure of bulge gage and its basic measuring principle

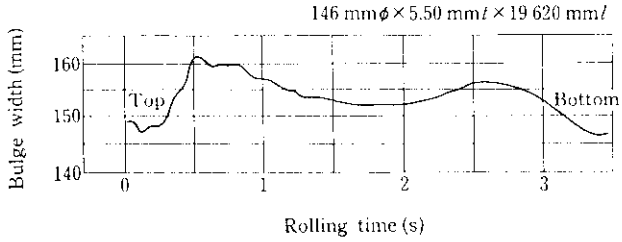


Fig. 7 An example of No. 4 stand outlet bulge width

distance. Therefore, the gage response must be 40 m/s or below.

(4) The measuring accuracy must be within ±0.5 mm, because the gages are used for mill control.

(5) The measuring environment is the hot rolling atmosphere with splashing of roll cooling water.

To satisfy the above-mentioned conditions, compact gages structured as shown in **Fig. 6** were developed. An actual measuring example using this bulge gage in the hot rolling line is shown in **Fig. 7**. The measuring result gave an accuracy of ±0.5 mm and a response of 35 ms, which completely satisfied the initial development aims. Further, this technique for the bulge gage was applied to the measurement of outside diameter of the hollow-bloom on the piercer delivery side, resulting in an effective utilization of development techniques.

## 5 Development of Rolling Control Model

### 5.1 Piercer[1)]

The piercer is a piercing-rolling mill which is located at the upmost-stream of the seamless tube rolling process. Therefore, the improvement in the dimensional accuracy of the pierced hollow bloom facilitates operations at downstream rolling mills, with full opportunities of the improvement in the dimensional accuracy of the final product.

At the piercer, the plug's outside diameter is first selected by the rolling schedule. Then, the gouge (barrel roll distance), the lead (plug tip position), the shoe distance, and the feed angle must be determined (refer to **Fig. 8**). The basic concept of the set-up model which determines these conditions was obtained by adopting the concept[2)] which had been developed for the 16″ seamless tube mill at Chita Works. Further, with the aims of improving the dimensional accuracy and achieving standardization, the plug which is used in circulation is tracked, and the tracking result is reflected on the adaptive control shown in **Fig. 9**. In the following, the concept of the model is explained.

As shown in Fig. 8, Eqs. (1) and (2) become valid geometrically.

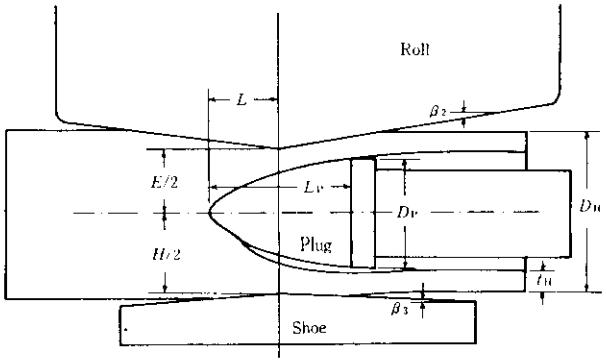


Fig. 8 Concept and notations of piercer

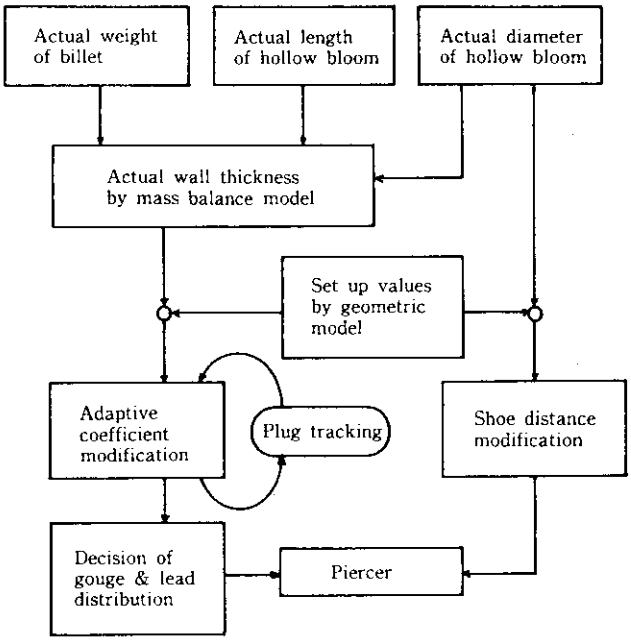


Fig. 9 Block diagram of piercing mill control model

$$\frac{E}{2} + (L_P - L)\tan\beta_2 = t_H + \frac{D_P}{2} \cdots\cdots\cdots (1)$$

$$D_H = a[H + 2(L_P - L)\tan\beta_3] + b[E + 2(L_P - L)\tan\beta_2] \cdots\cdots (2)$$

where $D_H$: Outside diameter of hollow bloom
$t_H$: Wall thickness of hollow bloom
$D_P$: Effective diameter of plug
$L_P$: Effective length of plug
$E$: Gouge distance
$L$: Lead distance
$H$: Shoe distance
$\beta_2, \beta_3$: Delivery-side angles of roll and guide-shoe
$a, b$: Coefficients

In general, the feed angle is determined by a factor other than hollow-bloom dimensions; hence, items

which require controlling are lead, gouge, and shoe distances. The outside diameter of the hollow bloom, when pierced into the same size, is strongly affected by the shoe distance. In piercing a billet into a hollow bloom, the dependability of the shoe distance on outside diameters changes, as shown in Eq. (3), depending upon the amount worked, namely, the wall thickness of the hollow bloom. Therefore, the wall thickness of the hollow bloom is used as control parameter. Next, the shoe constant which corresponds to the mill constant in flat products rolling is defined, and a feed-back model which uses this shoe constant as control gain is employed to control the outside diameter of the hollow bloom.

$$\Delta H = \gamma t_H (D_H^* - D_H) \quad \cdots\cdots\cdots\cdots\cdots (3)$$

where $\Delta H$: Shoe distance control amount
$\gamma$: Constant
$D_H^*$: Measured hollow bloom outside diameter

The follow bloom wall thickness is affected by the plug's effective diameter as can be seen in Fig. 8 or Eq. (1), if the gouge and lead distances are constant. Plugs are used in the circulation after their diameters are matched, but plug wear amounts are not uniform, depending upon the piercing conditions and the number of times of use. Namely, in actual cases, respective pieces are pierced by plugs having different diameters. In the following, the concept of the control model of hollow-bloom wall thickness is explained.

First, actual wall thickness $t_H^*$ of the hollow bloom which has been pierced by the $j$ th plug is obtained by Eq. (4).

$$t_H^*(j) = \frac{1}{2}\left(D_H^* - \sqrt{(D_H^*)^2 - \frac{4W_B^*}{\pi \rho_H l_H^*}}\right) \quad (4)$$

where $l_H^*$: Measured hollow bloom length
$W_B^*$: Billet weight after scale loss due to rotary furnace is taken into consideration
$\rho$: Density of steel at piercing temperature

Next, wall thickness compensation value $\Delta t_H^*$, which has taken into consideration the effects of plug's effective diameter and the mill constant, is obtained from the actual wall thickness by Eq. (5).

$$\Delta t_H(j) = t_H^*(j) + \frac{D_P}{2} - \frac{E}{2} - (L_P - L)\tan\beta_2 \cdots\cdots\cdots\cdots (5)$$

The value $\Delta t_H(j)$ is constantly tracked depending upon the number of times of use of the plug which is recirculated. Since the parameter which can control wall thickness is gouge or lead, wall thickness correction distribution coefficients $\alpha_1, \alpha_2$ ($\alpha_1 \geq 0, \alpha_2 \leqq 1$) can be used for obtaining Eqs. (6) and (7).[3]

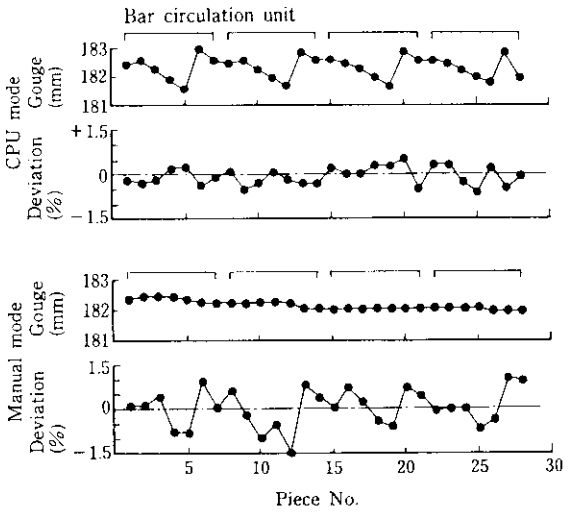


Fig. 10 Typical example between computer mode and manual mode

$$\Delta E(j \times j) = \alpha_1 \Delta t_H(j) + (1 - \alpha_1)\Delta L(j) \cdots (6)$$

$$\Delta L(j \times j) = \alpha_2 \Delta t_H(j) + (1 - \alpha_2)\Delta L(j) \cdots (7)$$

where $(j \times j)$ indicates that the same plug will be used at the next piercing chance in the plug circulation. **Figure 10** shows that as a result of piercing with the use of this control model, the deviation in the hollow bloom length is nearly halved compared with the result in manual piercing.

### 5.2 Mandrel Mill[4-7]

It has been said that the full-float mandrel mill is a rolling machine whose rolling phenomenon is the most difficult to explain for the following reasons:

(1) Since it is a three-dimensional rolling machine of the multi-stand type using grooved rolls, operation parameters are many in number and wide in the degree of freedom.
(2) It is impossible to observe or control the behavior of the mandrel bar during rolling, and fluctuations of bars to be used in circulation cause external disturbances to the rolling operation.
(3) The rolling time is shorter than that of flat products rolling, and the process is a continuous non-steady rolling at top and botton of the shell.

In developing the control model of this mill, the authors went back to the basic principle of rolling. First, the roll pass was improved, and pass shapes were made into numerical formulas. Next, the lubrication system of the internal surface of the shell and the mandrel bar was improved. Thirdly, a roll distance zero adjustment system was introduced in which pre-load was added to the roll, in order to minimize deviation of roll distances. The zero adjustment system reduced the scatter of the roll distances by a standard deviation of 0.1 mm and

improved roll setting accuracy. Through these improvements, the control environment was enhanced.

The roll pass at Chita Works was designed to reduce the wall thickness at the first-stage stands and to correct uneven thickness at the last-stage stands. Now the attention was focussed on the rolling load and shell cross-section mean wall thickness, and the difference between maximum and minimum values of these two factors in a single piece was measured. The result of mesured value for No. 5 stand is shown in **Fig. 11**. Similar result was obtained at No. 6 stand. As a result, it was confirmed that rolling load and wall thickness showed a good correspondence. Thus, to make the mean wall thickness of a single piece into a prescribed value and to make uniform the wall thickness distribution in the circumferential direction, a model was developed which would set up roll distances at the time of no load operation, so that rolling load would be predicted to make roll distances during rolling of all stands meet prescribed values and to make the respective odd-numbered and even-numbered wall-thickness-finishing stands into optimum values. **Figure 12** shows the outline of the control model for the shell cross section. In the following, the concept of the model is explained.

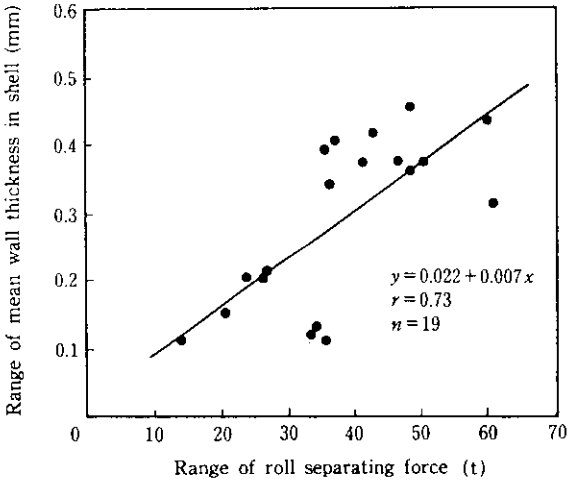


Fig. 11 Relation between wall thickness and roll separating force

First, the total rolling amount is obtained which is

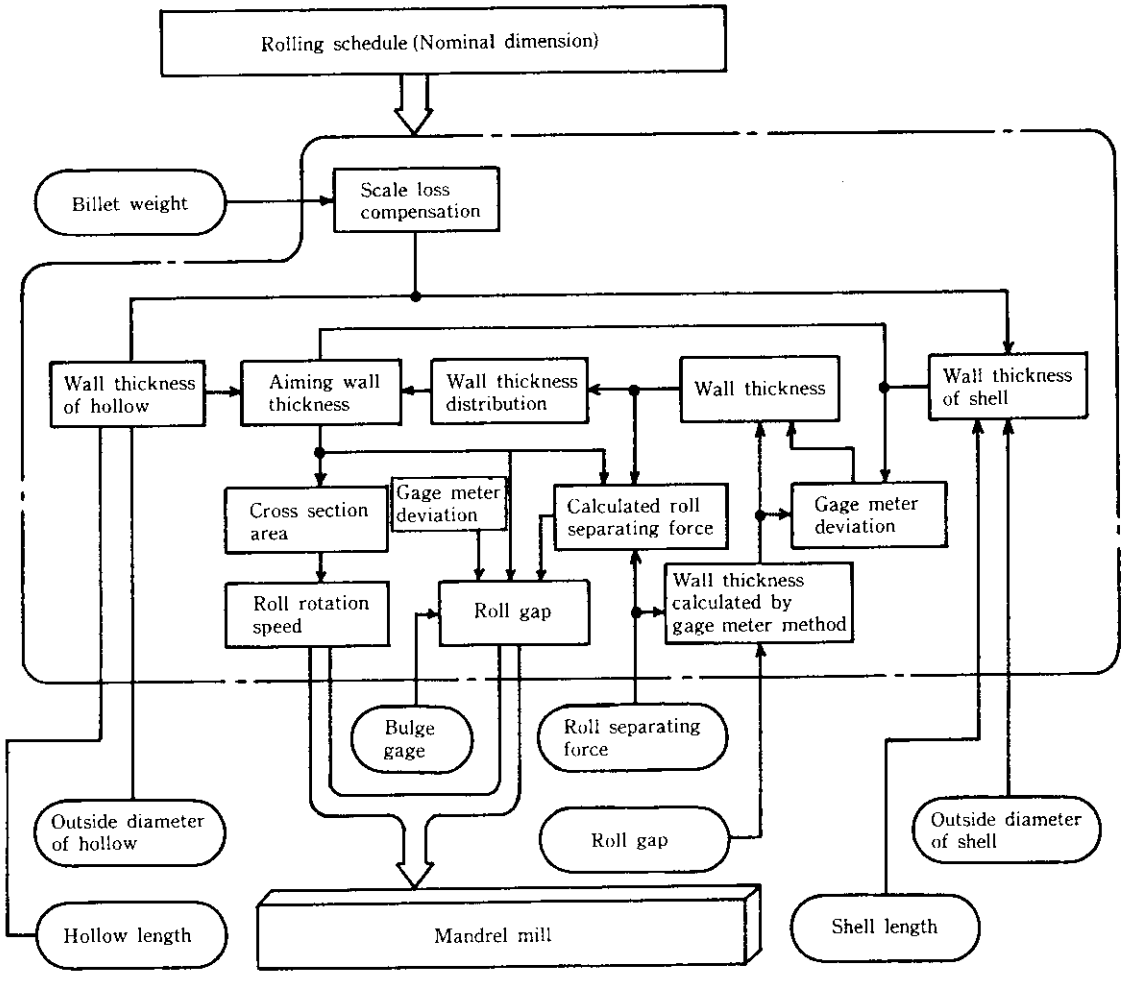


Fig. 12 Block diagram of wall thickness control for shell

required for rolling the actual hollow bloom wall thickness (entry side wall thickness) into the target shell wall thickness (delivery side wall thickness). Next, the rolling amounts at all the odd-numbered stands and even-numbered stands, namely, the reduced wall-thickness amounts are obtained. From these reduced wall-thickness amounts, a reduced wall-thickness quantity for each stand is calculated. At the same time, the reduced wall thicknesses of No. 5 and No. 6 stands, in particular, are optimized, so that the outlet wall-thickness distribution will become uniform in the circumferential direction.

Next, from these reduced wall-thickness amount, the bar temperature, and the hollow bloom temperature, it is possible to estimate the predicted rolling load, $\hat{P}(i)$, of each stand by regression and learning.

$$\hat{P}(i) = \left[a(i) + b(i)\left(1 - \frac{t_a(i)}{t_a(i-2)}\right)\right] \times C_P(i) C_B C_H \quad \cdots\cdots (8)$$

$$C_B = f_1(\theta_B) \quad \cdots\cdots (9)$$

$$C_H = f_2(\theta_H) \quad \cdots\cdots (10)$$

where $i$: Stand number

$C_P$: Learning coefficient of $i$-stand

$a, b$: Coefficients depending upon steel grades

$t_a(i)$: Delivery side wall thickness at $i$-stand

$\theta_B$: Measured bar temperature

$\theta_H$: Measured hollow bloom temperature

The rise in the bar temperature due to the circulating use of the bar will not bring about such great changes as to require the thermal expansion correction of the bar diameter, but the coating condition of the lubricant over the bar surface will change, and as a result, the friction coefficient between the internal surface of the shell and the bar surface will change. Since changes in the friction coefficient affect the prediction of the rolling load, the bar temperature is necessary as a control parameter. Also, since the hollow bloom temperature directly affects the deformation resistance, the temperature is necessary as a control parameter.

Next, the roll pass distance of each stand, namely, screw-down position $S(i)$, can be calculated from the predicted rolling load $\hat{P}(i)$, using Eqs. (11) and (12).

$$S(i) = (D_B - \Delta G) + 2t_a(i) - \frac{\hat{P}(i) - P_0}{M} \quad \cdots\cdots (11)$$

$$t_a(i) = t_a(i-2) - \Delta t_a(i) \quad \cdots\cdots (12)$$

where $D_B$: Bar outside diameter

$\Delta G$: Wall thickness deviation by the gage meter method

$\Delta t_a(i)$: Reduced wall-thickness amount at $i$-stand

$P_0$: Preloaded load value at zero adjustment

$M$: Mill constant

Now that screw-down positions of rolls of all stands have thus been determined, the rotation of the roll, $N(i)$, will be determined next. The roll rotation is determined by the mass-flow constant law from the relation between the shell sectional area and the roll neutral point, so that the inter-stand tension will become an optimum value.

In the present shell cross section shape control model, it is considered that the screw-down position of rolls is main, and the roll rotation is subordinate.

Rolled shells are identified by such measured values as the shell length $l_s$*, the rolling load $P(i)$, and the bulge width values at No. 4 and No. 7 stands. From the rolling load, the actual wall thickness of each stand is calculated by the gage meter method.

$$t(i) = \frac{G(i) - D_B}{2} \quad \cdots\cdots (13)$$

Here $G(i)$ is the roll caliber distance during rolling and expressed by Eq. (14).

$$G(i) = S(i) + \frac{P(i) - P_0}{M} \quad \cdots\cdots (14)$$

Next, the wall thickness deviation $\Delta G$ is calculated. The wall thickness deviation is obtained from Eq. (15) using actual wall thickness value $t(5)$ and $t(6)$ at No. 5 and No. 6 stands, which are wall thickness finishing stands, and measured shell wall thickness $t_s$*.

$$\Delta G = \Delta G^{l-1} + 2\left(t_s^* - \delta \times \frac{t(5) + t(6)}{2}\right) \quad (15)$$

where $\delta$: Constant determined by tube size

In Eq. (15), $\Delta G^{l-1}$ is the wall thickness deviation of one former circulation, that is, the wall thickness deviation when the same bar was used in the next preceding rolling. Actual shell wall thickness is obtained by Eq. (16).

$$t_s^* = \frac{1}{2}\left(D_s^* - \sqrt{(D_s^*)^2 - \frac{4W_B^*}{\pi \rho_s l_s^*}}\right) \quad \cdots\cdots (16)$$

Here actual shell outer diameter $D_s$* is defined as follows: Since the outside diameter shape of the shell is ordinarily an ellipse, the longer side will be the bulge, and the shorter side will be $G(i)$, namely, the roll pass distance during rolling. From the circumference approximation formula of the ellipse, a shell's circumferential length is obtained, thereby deriving an outside diameter which has been converted into the true circle.

Next, wall thickness correction value $t_c(i)$ is calculated for the next following screw-down position correction at each stand. This value can be obtained by Eq. (17)[8,9] using the formula.

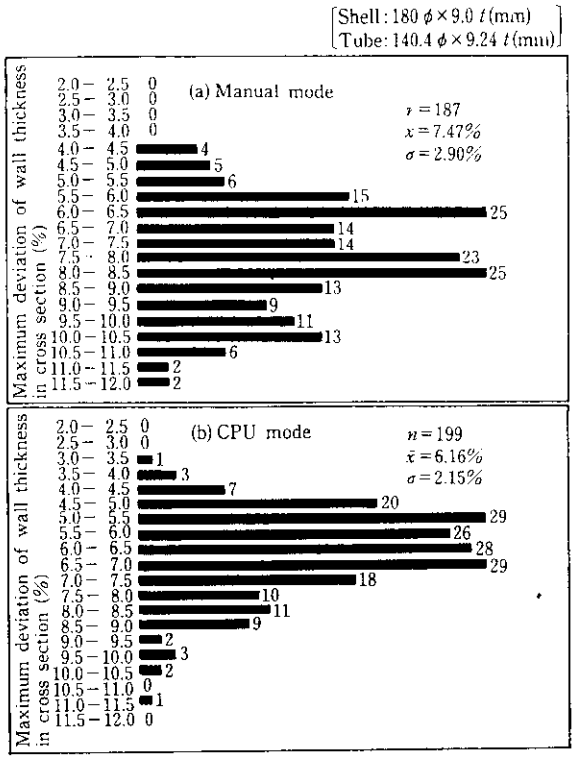


Fig. 13 Comparison of wall thickness deviation in cross section after stretch reducer between manual mode and computer mode

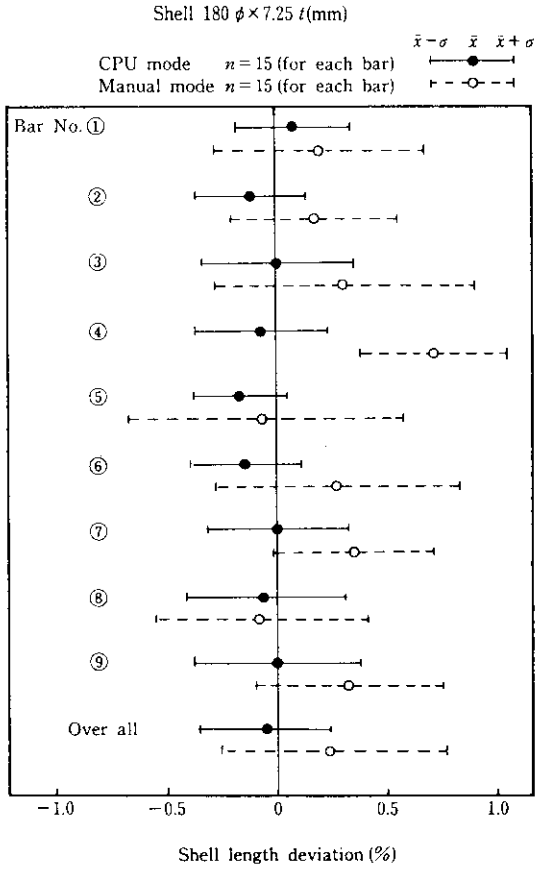


Fig. 14 Comparison of shell length deviation between manual mode and computer mode

$$t_c(i) = t(i) + \frac{\Delta G}{2} \quad \cdots\cdots\cdots\cdots\cdots\cdots (17)$$

Through the use of this wall thickness correction value, a predicted rolling load for the next piece is obtained by Eq. (8), and the screw-down position of the roll by Eq. (11). From the screw-down position of the roll obtained by Eq. (11) and the roll pass, the bulge width is predicted, and it is confirmed that the screw-down position is within a range free from the generation of bulge-type[10] flaw. The above procedure is repeated.

The above is the mandrel mill sectional shape control model. An example of improvement in the wall thickness deviation in the cross section as a result of rolling with this model is shown in **Fig. 13**, and an example of similar improvement in the elongation length, that is, mean wall thickness is shown in **Fig. 14**. The wall thickness deviation in the cross-section shows an improvement of about 1%, and the scatter of the mean wall thickness shows an improvement of from 0.5% to 0.3% in a standard deviation. Further, the generation of bulge-type flaws has been completely eliminated.

### 5.3 Stretch Reducer

The stretch reducer means a reducing mill, which finishes the tube's outside diameter into the prescribed size. Contrary to the mandrel mill, the stretch reducer has no tool to roll the internal surface of the tube. It has no screw down system either, because three rolls are arranged in 120° directions as shown schematically in Fig. 4. According to the theory by Neumann-Hanke[11], the reduction of the tube's outside diameter using grooved rolls increases wall thickness and elongates the tube in the lengthwise direction. To finish wall thickness into the prescribed thickness value, therefore, it is necessary to control the wall thickness while giving the tension to the tube. To apply the optimum tension to the tube, the roll rotation must be controlled.[12] Hence, an optimal elongation control model shown in **Fig. 15** has been developed. In the following, the concept of this model is explained:

At the stretch reducer, the tube's outside diameter on the entry side and finished outside diameter of the tube to be rolled are given beforehand. Therefore, the grooved roll arrangement is determined according to the outside diameter reduction ratio. Thus, the mean stretch coefficient can be obtained by the aforesaid Neumann-Hanke's theoretical formula, that is Eq. (18).

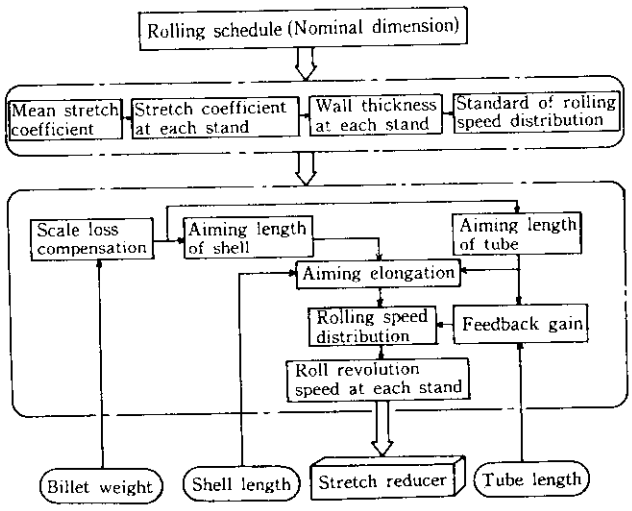


Fig. 15 Block diagram of tube length control

$$\frac{2Z(\lambda-1)+(1-2\lambda)}{\varphi_r} = \frac{Z(1-\lambda)+(1+\lambda)}{\varphi_l} = \frac{Z(1-\lambda)+(2+\lambda)}{\varphi_\theta} \quad \cdots\cdots(18)$$

where $Z$: Mean stretch coefficient (tube axial-direction stress/deformation resistance)
$\lambda$: Wall thickness/outside diameter
$\varphi_r$: Radial-direction logarithmic distortion of tube
$\varphi_l$: Lengthwise-direction logarithmic distortion of tube
$\varphi_\theta$: Tangential-direction logarithmic distortion of tube

The mean stretch coefficient is distributed over stretch coefficients between all stands. From the stretch coefficients and tube's outside diameters in the entry and delivery sides at all stands, wall thickness values on the delivery side at these stands can be calculated. From the tube's outside diameters and the wall thickness on the entry and the delivery side of a stand, the circumferential speed of the roll is obtained by applying the mass flow constant law, thereby determining the roll rotation.

From the rolling schedule, the reference elongation $E_0$ at the stretch reducer is determining by Eq. (19).

$$E_0 = \frac{t_S(D_S - t_S)}{t_T(D_T - t_T)} \quad \cdots\cdots(19)$$

The target length of the tube is calculated from Eq. (20), and the ratio between the target length of the tube and tube length $l_T$ indicated in the rolling schedule is obtained. Then the ratio between the target length of shell $l_{SA}$ obtained from Eq. (21) and the measured length of shell $l_S$* is obtained.

$$l_{TA} = \frac{W_B^*}{\pi\rho_T t_T(D_T - t_T)} \quad \cdots\cdots(20)$$

$$l_{SA} = \frac{W_B^*}{\pi\rho_S t_S(D_S - t_S)} \quad \cdots\cdots(21)$$

Next, elongation $E'$ of the tube to be rolled is calculated by Eq. (22).

$$E' = E_0\left(\frac{l_{SA}}{l_S^*}\right)\left(\frac{l_{TA}}{l_T}\right) \quad \cdots\cdots(22)$$

To find the tube's elongation ratio, when the elongation changes, a regression formula shown in Eq. (23), which uses the stretch coefficient as a parameter, has been prepared.[13,14]

$$\Phi = uZ(E-1)^{vZ} \quad \cdots\cdots(23)$$

where $u, v$: Coefficients

If the rotation of the stretch reducer rolls changes linearly with respect to the reference stand, it will be most simplified. Therefore, the correction quantity of the roll rotation is calculated by Eq. (24).

$$\frac{\Delta N(i)}{N(i)} = \frac{\Phi(E') - \Phi(E_0)}{\Phi(E_0)} \times \frac{i}{24} \quad \cdots\cdots(24)$$

where $\Delta N$: Roll rotation correction quantity
$N$: Reference roll rotation

When rolling is finished, tube length $l_T$* can be measured, and therefore, it is so designed that Eq. (23) can be learned and, further, the accuracy of the regression formula model can be improved.

The comparison between the target length and the measured length of the tube, when rolling is performed according to the optimum elongation model and when rolling is performed manually by the operator, is shown in **Fig. 16**, which clearly indicates that the tube length deviation, when rolling is performed using the newly developed model, has greatly improved in the mean value and the standard deviation compared with manual rolling.

## 6 Results of Application

In the above, the contents of various mill control models were explained. Some of these models were developed in parallel with the development of sensors, resulting in some difficulties in process applications.

The application of the computer mode to the mill was advanced in synchronization with the completion of model development, and was sequentially incorporated into processes starting from the downstream i.e. stretch reducer. As an example, the transition of the computer mode application ratio to the stretch reducer is shown in **Fig. 17**. At present, the computer mode operation has been firmly established at all mills.

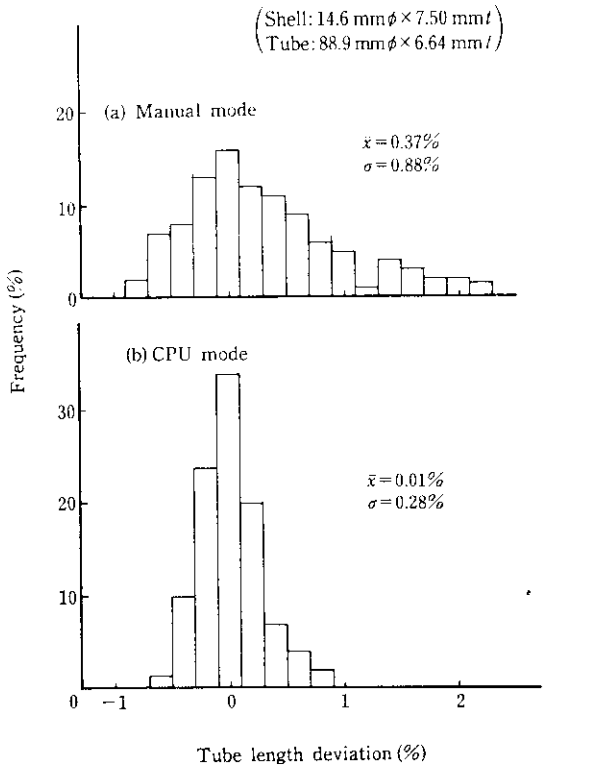


Fig. 16 Comparison of tube length deviation between manual mode and computer mode

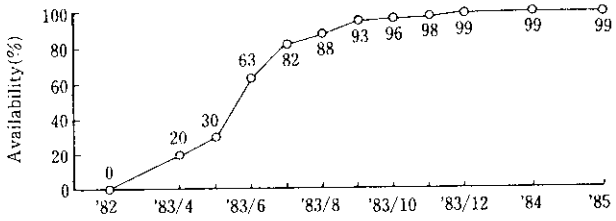


Fig. 17 Availability of computer mode rolling for stretch reducer

Partial achievements of these applications were described in the explanation of the control models for each mill, and as a consolidated outcome throughout the entire operation, the following were observed:

(1) The effect of dimensional accuracy improvement by the mill control models was so noticeable that yield improvement was 0.4%, and the bulge-type flaw was completely eliminated.
(2) The productivity has shown about 10% improvement owing to full-automation of mill presetting and the adoption of the material tracking system.
(3) Because of item (2) above and the unification of operators' rooms, about 10% labor saving has been attained.

Further, the fundamental effect was embodied in the thoroughgoing standardization of the operation with the development and the introduction of the control systems. Through this standardization, the level of the quality of the operation has been upgraded. Further, functions such as the automatic collection and analysis of on-line data have expedited various development projects and tests at the mill and, in combination with the aforesaid material tracking system, have greatly contributed to strengthening of the quality assurance system.

## 7 Conclusions

With the aim of improving the quality and the productivity of seamless steel tubes, a 7″ seamless steel tube rolling control system was developed in 1983 and it has been sequentially incorporated into actual production processes. As a result of the aforesaid developments of control systems, on-line gages and rolling models, a noticeable outcome has been achieved such as a yield improvement of 0.4%, and the productivity improvement and the labor saving, respectively, of about 10%.

However, the environment, surrounding seamless steel tubes, has turned more and more rigorous in recent years, and to cope with such a condition, the rolling control techniques require further upgrading of their levels. The authors intend to carry out the development of new high-response sensors, development of precision models and dynamic models which will actively utilize the plasticity theory and control theory, and the intensification of the control system in the future.

Finally, the authors express their deep appreciation to those who have kindly rendered valuable cooperation in the course of development of the present system.

### References

1) Kawasaki Steel Corp.: Jpn. Kokai 57-115907
2) Y. Sayama, H. Tomigashi, A. Ejima, Y. Funyu, K. Sakurada, T. Maguchi, and Y. Taguchi: *Kawasaki Steel Giho*, **13**(1981)1, 1-13
3) Kawasaki Steel Corp.: Jpn. Kokai 60-137516
4) T. Okamoto and C. Hayashi: *Sumitomo Metals*, **23**(1971)4, 441
5) M. Kamata, M. Okato, Y. Mihara, F. Fujita, T. Hirakawa, and M. Numano: *Nippon Kokan Technical Report*, 101(1984), 22-34
6) C. Hayashi, T. Yamada, M. Utakhoji, and F. Hirao: *J. of JSTP*, **24**(1983)273, 1078-1985
7) N. Konya, H. Oka, S. Okumura, and Y. Funyu: Proceedings of the 1985 Japanese Spring Conference for the Technology of Plasticity, 122, (1985)
8) Kawasaki Steel Corp.: Jpn. Kokai 60-240323
9) Kawasaki Steel Corp.: Jpn. Kokai 60-64712
10) Kawasaki Steel Corp.: Jpn. Kokai 59-78704
11) Neumann U. Hanke: *Stahl u. Eisen*, **75**(1955)22, 1452
12) T. Yamada: *J. of the Japanese Soc. of Mechanical Engineers*, **83**(1980)740, 30-36
13) Kawasaki Steel Corp.: Jpn. Kokai 58-128209
14) Kawasaki Steel Corp.: Jpn. Kokai 60-21114